Korean J. Chem. Eng., 32(9), 1713-1719 (2015)
DOI: 10.1007/s11814-015-0147-2
pISSN: 0256-1115
eISSN: 1975-7220

INVITED REVIEW PAPER

Integrated fabrication-conjugation approaches for biomolecular assembly and protein sensing with hybrid microparticle platforms and biofabrication - A focused minireview

Sukwon Jung and Hyunmin Yi†

Department of Chemical and Biological Engineering, Tufts University, 4 Colby St. Medford, MA 02155, U.S.A.
(*Received 22 May 2015 • accepted 5 July 2015*)

Abstract−Controlled manufacturing of polymeric hydrogel microparticles is crucial, yet challenging, for rapid and sensitive detection of biomacromolecules in biodiagnostics and biosensing applications. Our approach is an integrated fabrication-conjugation strategy utilizing a simple and robust micromolding technique and biofabrication with a potent aminopolysaccharide chitosan as an efficient conjugation handle for high-yield bioorthogonal conjugation reactions. We present a concise overview of our recent findings in the controlled fabrication of shape-encoded or core-shell structured microparticles consisting of poly(ethylene glycol) (PEG) and short single-stranded (ss) DNA or chitosan, and their utility in the covalent conjugation and nucleic acid hybridization-based assembly of target ssDNAs, proteins and viral nanotemplates. Particularly, two novel routes to achieve substantially improved protein conjugation capacity and kinetics are presented from our recent reports: tobacco mosaic virus (TMV) as a high capacity nanotubular template and polymerization-induced phase separation (PIPS) of pre-polymer droplets for controlled core-shell structure formation. We envision that our fabrication-conjugation approaches reported here, combined with our current and future endeavors in improved fabrication and design of controlled structures with chemical functionalities, should permit a range of manufacturing strategies for advanced functional microscale materials and platforms in a wide array of applications.

Keywords: Micromolding, Hydrogel Microparticles, Biofabrication, Biomolecular Conjugation, Biosensing

INTRODUCTION

Rapid and reliable detection of biomacromolecules is essential in a number of application areas, including medical diagnostics, biological threat detection, and biopharmaceutical process control [1-3]. Traditional technologies include planar microarrays, bead-based assays and enzyme-linked immunosorbent assay (ELISA). While offering high-throughput capability, planar and bead arrays face challenges in rapid and reliable detection. These include low probe titer due to limited number of probes on surfaces, long and complex incubation and rinsing procedures due to nonspecific adsorption, and costly equipment both for fabrication of the sensing platforms and detection of analytes. While still being considered the gold standard, ELISA has also limitations, such as the large number of samples needed and false positive signals arising from nonspecific adsorption as well as its lengthy and laborious procedures.

Suspension arrays of polymeric hydrogel microparticle platforms offer many advantages in addressing these challenges in traditional materials and methods. The hydrophilic and often non-fouling nature of hydrogels provides selective probe-target interactions while offering enhanced probe titer and small assay volume along with reduced needs for extensive rinsing [4-6]. Further, rapid binding and short incubation periods could permit near-real time detection for on-site diagnostics or on-line bioprocess control. Recent advances in the fabrication of hydrogel microparticles for biosensing applications have led to promising technologies that offer complex encoding schemes based on shapes and colors. Such techniques include photolithography [7-9], droplet-based polymerization [10-12] and flow lithography [13,14] in microfluidic devices. The photolithographic methods adopted from semiconductor industry have been utilized for manufacture of simple shape-encoded hydrogel particles [7-9]. While this technique is facile and convenient, there exist limitations in particle uniformity (i.e., particle sizes and features). The emerging microfluidics-based fabrication strategies have allowed for manufacture of highly uniform hydrogel microparticles with a great number of graphical or spectral codes [10-14]. Yet, these techniques also face limitations in delicate control of fabrication parameters, need for complex and costly equipment, and lack of scalability.

Our approach to addressing these limitations involves seamless integration of robust micromolding-based fabrication of PEG-based polymeric hydrogel microparticles with controlled structures (i.e., simple shape-encoded or core-shell architectures), biopolymeric conjugation handles and high-yield bioorthogonal reactions in a post-fabrication conjugation fashion. First, the soft lithography-based micromolding techniques allow for fabrication of monodisperse and well-defined hydrogel microparticles in a simple and robust manner without any delicate controls and complex devices. In addition, due to the batch processing-based nature of the micromold-

†To whom correspondence should be addressed.
E-mail: hyunmin.yi@tufts.edu

ing techniques, these methods are readily scalable and flexible in enlisting a large range of fabrication parameters. Second, stable incorporation of biopolymeric materials such as single-stranded (ss) DNA and chitosan with the hydrogel microparticles provides efficient conjugation handles that enable further assembly of functional biomolecules, hence, the term "biofabrication." Specifically, the ssDNAs modified with methacrylate functional groups are co-polymerized during particle synthesis, and allow nucleic acid hybridization-based biomolecular assembly. The chitosan molecules are incorporated with the particles and provide chemically reactive sites by utilizing abundant primary amine groups with uniquely low pKa value (~6.4) on their backbones. Third, bioorthogonal reactions enable highly selective and efficient bioconjugation by exploiting functional groups that do not exist in nature, unlike conventional conjugation schemes. In addition, our post-fabrication conjugation approach permits retention of the activities of labile biomolecules (e.g., antibodies) by preventing their potential damage during particle fabrication. In this focused minireview, we also describe our two recent efforts to overcome limited probe titer and slow mass transfer of biomacromolecules in non-macroporous polymer networks. First, tobacco mosaic virus (TMV) nanotemplates offering abundant conjugation sites assembled on surfaces of non-macroporous microparticles via nucleic acid hybridization provide less hindered mass transport environment. Second, microparticles consisting of macroporous polymer networks were fabricated via a micromolding technique utilizing surface tension-induced droplet formation.

Combined, these integrated fabrication-conjugation strategies offer simple routes for controlled manufacturing of biomolecular assembly and biosensing platforms with enhanced capabilities over traditional platforms. We thus envision that our strategies can be readily enlisted in a wide range of biosensing application areas.

ROBUST REPLICA MOLDING (RM)-BASED FABRICATION OF DNA-CONJUGATED HYDROGEL MICROPARTICLES

Our first effort in harnessing the robust soft-lithographic micromolding technique for controlled fabrication of biosensing microparticle platforms involved replica molding (RM) of DNA-conjugated PEG microparticles with simple shape-encoding [15], as shown in Fig. 1. Specifically, an aqueous mixture of polymerizable PEG diacrylate (PEGDA), methacrylate-modified (Acrydite™) single-stranded (ss) DNA and a photoinitiator (2-hydroxy-2-methylpropiophenone, Darocur 1173) is added to 2D-shaped microwells made of poly(dimethylsiloxane) (PDMS) elastomer, prepared via a simple lift-off from photolithographically patterned silicon mastermolds in the first step of our RM scheme (Fig. 1(a)). These microwell patterns are sealed with thin PDMS-coated glass covers to prevent evaporation, and UV light at 365 nm irradiated with a simple hand-held UV lamp (8 W) for photoinduced radical polymerization. Simple bending of the micromolds then yields near-complete recovery of the monodisperse microparticles co-polymerized with the Acrydite™-ssDNAs, permitting reliable replication of 2D shapes. Bright-field and fluorescence micrographs of mixtures of the as-prepared ssDNA-conjugated microparticles with three distinct shapes and

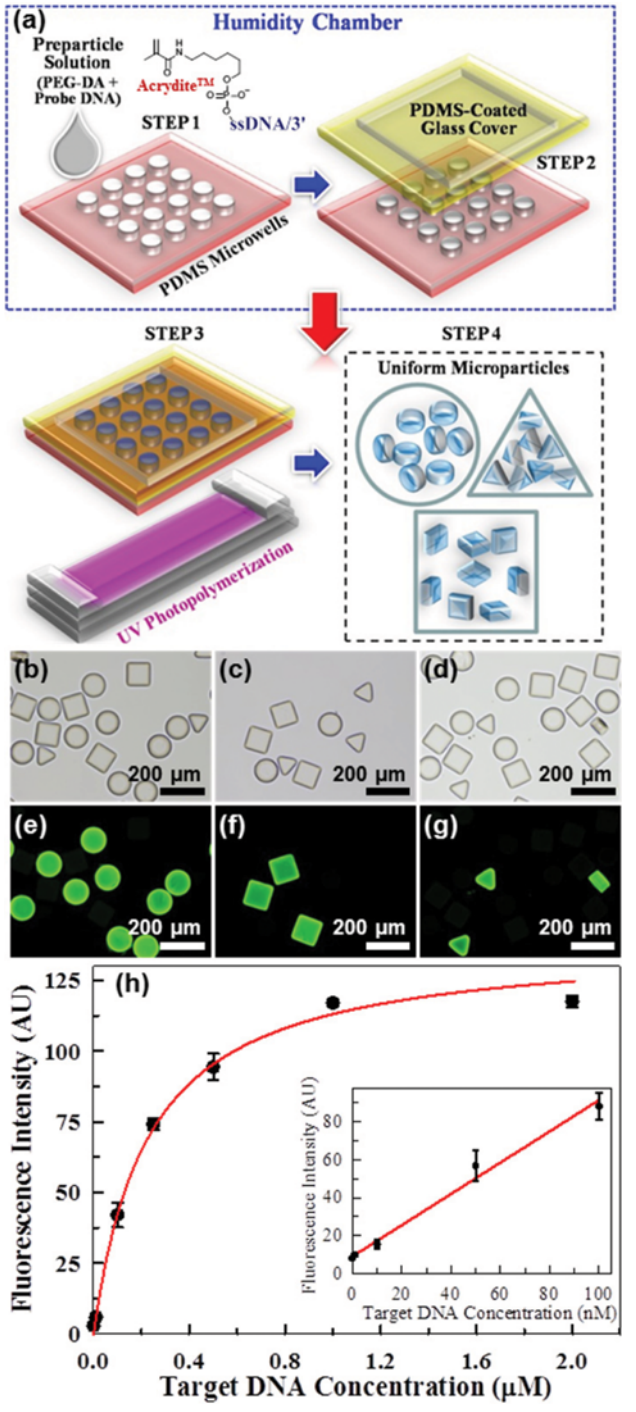

Fig. 1. Fabrication of ssDNA-conjugated hydrogel microparticles via RM. (a) Schematic diagram of the RM-based microparticle fabrication. (b)-(d) Bright-field micrographs of three different probe ssDNA-conjugated microparticles that are encoded with three different shapes. (e)-(g) Fluorescence micrographs of mixtures of shape-encoded probe ssDNA-conjugated microparticles corresponding to the bright-field images in (b)-(d) upon hybridization with fluorescently labeled target ssDNAs with sequences complementary to probe ssDNA for each particle shape. (h) Responsiveness of the ssDNA-conjugated microparticles with varying target ssDNA concentrations. Adapted from [15]. Copyright (2010) American Chemical Society.

probe ssDNA sequences in Fig. 1(b)-(g) clearly showed the simple shape-based encoding upon hybridization with fluorescently labeled target ssDNA molecules with matching sequences. Further examination of the responsiveness of these microparticles with target ssDNA concentration yielded typical Langmuir isotherm-type saturation behavior (Fig. 1(h)), with linear increase in the fluorescence intensity at low target concentration. Importantly, these results illustrated several advantages of our RM-based approach including the inherently simple, clean and robust replication of functional hydrogel microparticles with 2D shapes, facile and flexible fabrication parameter control, and minimal waste of precious materials (e.g., ssDNA). Meanwhile, confocal microscopy results showed limited penetration depth (~5.5 μm) of the target ssDNAs (~6 kDa, Rg ~2 nm) [16] through the non-macroporous PEG networks, indicating limited mass transfer of the relatively small biomacromolecular targets (data not shown) [15]. In short summary, this first report demonstrated that a simple RM can be enlisted for fabrication of biofunctional microparticles with controlled shapes and uniform morphologies.

BIOMOLECULAR CONJUGATION WITH CHITOSAN-PEG MICROPARTICLE PLATFORMS AND SPAAC REACTION

Next, we extended this simple RM-based fabrication scheme to manufacture PEG-based microparticles containing chitosan [17], as shown in Fig. 2. Similar photopolymerization of a simple mixture of PEGDA and short-chain chitosan in 2D-shaped micromolds led to fabrication of uniform microparticles in a shape-controlled manner as shown in the schematic diagram and bright-field micrographs of Fig. 2(a). Chitosan is a naturally derived aminopolysaccharide obtained by deacetylation via boiling in alkaline conditions from chitin, a linear polymer of *N*-acetylglucosamine and the primary structural component of crustaceans such as crabs, shrimps and insects. Depending on the degree of deacetylation, up to 99% of each monomeric unit of chitosan results in glucosamine with a primary amine group with a uniquely low pK_a value of ~6.4 (chitosan scheme in Fig. 2(a)) [18]. This primary amine group is thus positively charged in acidic conditions, providing repulsive forces among the glucosamine monomeric units and rendering solubility in aqueous solutions. At higher pH ranges, the amine groups become neutral/uncharged, and long chain chitosan often becomes insoluble in water. Due to this pH-responsive charge transition along with several gelation approaches including physical association (hydrophobic interaction, hydrogen bonding or crystallization), complexation (with anions or metal ions) and chemical crosslinking, chitosan has widely been exploited to construct functional materials for a variety of applications, including tissue engineering, drug delivery, and chemical and biosensing [18-21]. Importantly, the unshared electron pair of the chitosan's primary amines under neutral conditions is highly nucleophilic unlike lysine's amines (pK_a ~10.5 [22], positively charged under most conditions), thus providing efficient handles for amine-reactive conjugation reactions. For example, the schematic diagram and fluorescence micrographs of Fig. 2(b)-(e) show that the chitosan-PEG microparticles undergo amidation reaction with an amine-reactive *N*-hydroxysuccinimidyl ester form

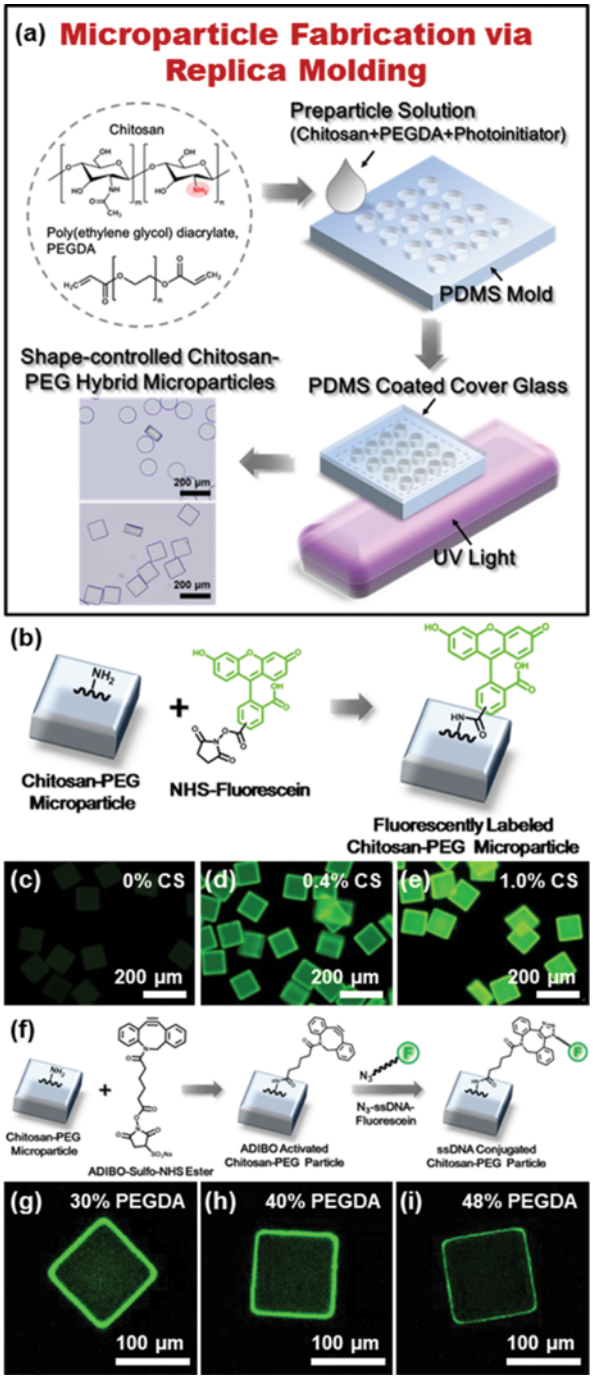

Fig. 2. Fabrication of chitosan-PEG hybrid hydrogel microparticles via RM. (a) Schematic diagram of the microparticle fabrication procedure via RM, and bright-field images of the as-prepared chitosan-PEG microparticles. (b) Schematic diagram for fluorescent labeling of chitosan-PEG microparticles via amidation reaction. (c)-(e) Fluorescence micrographs of the microparticles (c) without and (d), (e) with chitosan upon incubation with amine-reactive fluorescein molecules. (f) Schematic diagram of ssDNA conjugation with the chitosan-PEG microparticles via SPAAC reaction. (g)-(i) Confocal micrographs of the microparticles containing different PEG contents upon conjugation with azide-modified and fluorescently labeled ssDNAs. Adapted from [17] and [23]. Copyright (2012 & 2013) American Chemical Society.

of fluorescein, confirming the retained chemical reactivity of the incorporated chitosan. Further FTIR and long-term storage experiments also confirmed stable incorporation of chitosan, presumably due to the covalent amine-radical reaction [17]. We then utilized bioorthogonal strain-promoted alkyne-azide cycloaddition (SPAAC) reaction to conjugate azide-modified and fluorescently labeled ssDNA onto the azadibenzocyclooctyne (ADIBO)-activated chitosan-PEG microparticles, as shown in Fig. 2(f)-(i). Importantly, relatively large size of the ssDNA allowed the examination of the penetration depth and mesh size of the microparticles prepared with varying PEG content, as shown in the confocal micrographs of Fig. 2(g)-(i). The as-conjugated ssDNAs then served as anchoring handles for TMV templates via hybridization, as further discussed in Section 5. In short, this work demonstrated a simple fabrication method to produce uniform biopolymeric-synthetic hybrid microparticles with abundant chemical functionality via RM, as well as the utility of the chitosan moieties for efficient biomacromolecular conjugation via SPAAC reaction.

PROTEIN CONJUGATION AND CAPTURE KINETICS

We then extended this fabrication-conjugation scheme to examine protein conjugation and antigen-antibody binding behavior using a bright red fluorescent protein R-phycoerythrin (R-PE) and anti-R-PE antibody (Ab) using the SPAAC reaction [23], as shown in Fig. 3. First, bright fluorescence on the microparticles (Fig. 3(a)-(c)) indicates conjugation of azide-modified fluorescence molecules (i.e., fluorescent markers, fluorescein labeled single-stranded DNAs and R-PEs) via SPAAC reaction, regardless of their sizes. Next, confocal micrographs taken at the center of the microparticles in Fig. 3(d)-(f) show decreasing penetration depth of the conjugated molecules as the molecular weight increases from full penetration for a small fluorescent marker (F-488, MW 576 Da) to ~3 μm for R-PE (MW 240 kDa). Careful examination of the protein conjugation kinetics in Fig. 3(g) revealed three regimes. Initially, the protein conjugation with the microparticles proceeds rapidly (three times faster than the reaction between small molecules in a bulk solution) due to multiple conjugation sites on both the azide-modified proteins and the ADIBO-activated sites in the pores of microparticles. As the proteins become conjugated and block the path for diffusion, the apparent conjugation rate decreases as indicated by the dotted line. Finally, we examined the Ab-Ag binding kinetics between anti-R-PE Ab-conjugated microparticles and target R-PEs as shown in Fig. 3(h). Near-complete binding within the first 15 min was observed at high R-PE concentration conditions, suggesting potential for near-real time monitoring of biopharmaceutical processes [1]. Combined with simple shape-based encoding for multiplexed assays (see Fig. 5 in reference [23]), this study provided detailed analysis on the effects of large protein sizes on apparent biomolecular conjugation kinetics.

ENHANCED PROTEIN CONJUGATION AND CAPTURE WITH VIRAL NANOTEMPLATES

As shown in the limited penetration of biomolecules and slow conjugation kinetics due to hindered mass transfer (Fig. 3), non-

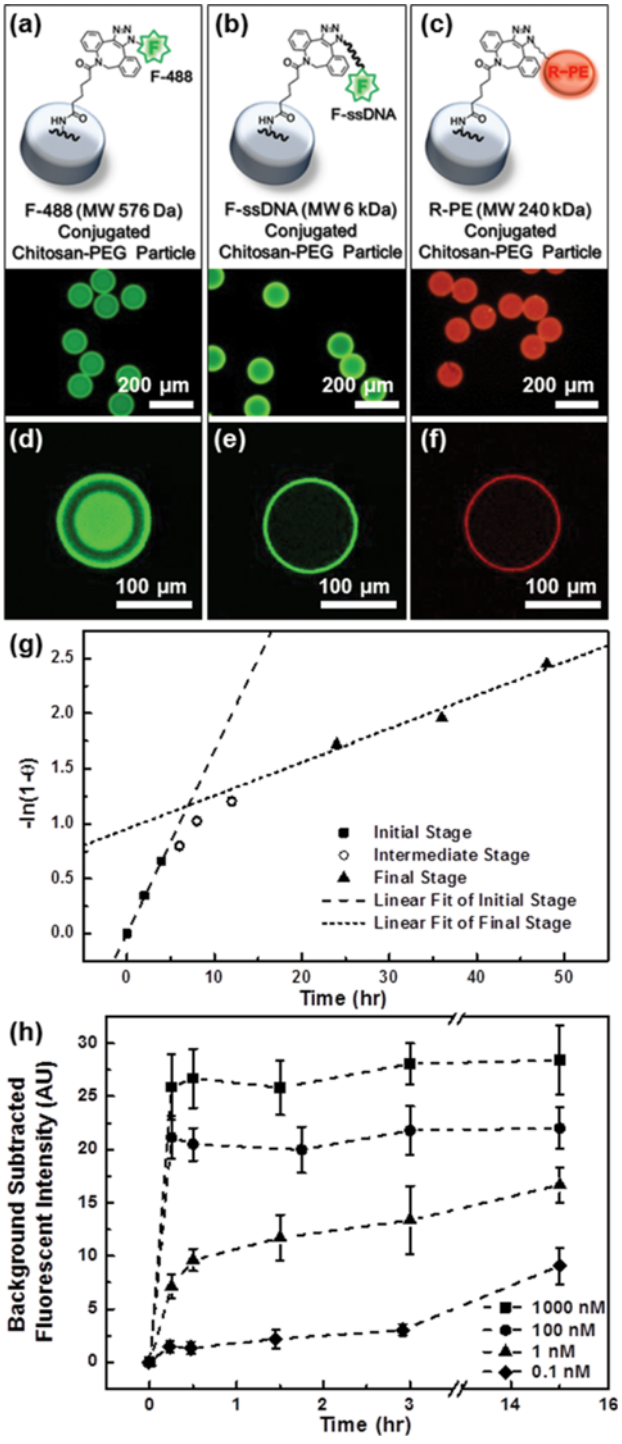

Fig. 3. Protein conjugation and capture with chitosan-PEG microparticles. (a)-(b) Schematic diagram (top row) and fluorescence micrographs (bottom row) of chitosan-PEG microparticles conjugated with different sized fluorescent molecules via SPAAC reaction; (a) small fluorescent marker (F-488), and relatively large (b) ssDNA and (c) red fluorescence protein R-PE. (d)-(f) Confocal micrographs of the microparticles corresponding to those shown in (a)-(c). (g) Protein conjugation kinetics with the chitosan-PEG microparticles via SPAAC reaction. (h) Target protein binding kinetics with antibody-conjugated chitosan-PEG microparticles. Adapted from [23]. Copyright (2013) American Chemical Society.

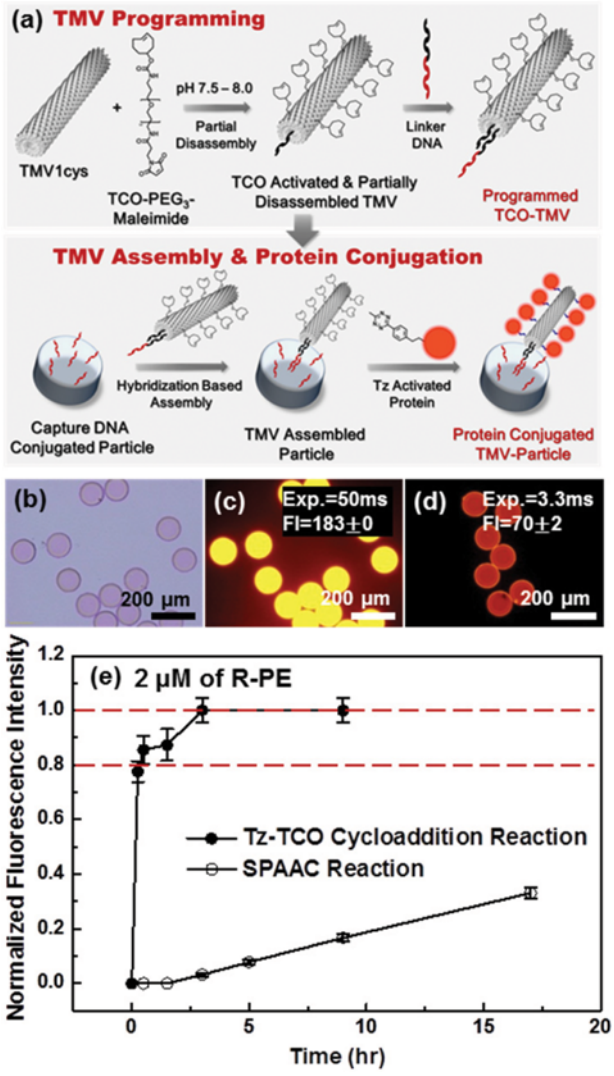

Fig. 4. TMV-assembled chitosan-PEG microparticles (TMV-particles) for improved protein conjugation. (a) Schematic diagram of TMV functionalization, partial disassembly and nucleic acid hybridization-based assembly with the chitosan-PEG microparticles. (b)-(d) R-PE conjugated TMV-microparticles: (b) bright-field micrographs, and (c), (d) fluorescence micrographs under different imaging conditions. (e) R-PE conjugation kinetics with TMV-microparticles via Tz-TCO (solid circles) and SPAAC (open circles) reaction. Adapted from [24]. Copyright (2014) American Chemical Society.

macroporous hydrogel microparticle platforms have limitations in probe capacity and conjugation/binding kinetics. Our first attempt in addressing this limitation harnessed nanotubular viral templates [24], as shown in Fig. 4. Specifically, partial disassembly at the 5′-end of genetically modified tobacco mosaic virus (TMV1cys) templates allows the nucleic acid hybridization-based assembly through its genomic mRNA sequence in a mild and orientationally controlled manner, while the genetically displayed cysteines near outer edge of each coat protein provide thiol moiety for efficient maleimide-based conjugation, as shown in the schematic diagram of Fig. 4(a). In this work, we utilized another bioorthogonal conjugation reaction, rapid tetrazine-trans-cyclooctene (Tz-TCO) reaction to examine the utility of TMV templates for high capacity probe titer and improved mass transfer; each TMV possesses over 2000 identical coat proteins (thus thiol functionality). As partially evidenced by the bright-field and fluorescence micrographs of Fig. 4(b)-(d), TMV-assembled microparticles exhibited 53-fold enhancement in protein conjugation capacity over chitosan-PEG microparticles (Fig. 3) as well as much improved conjugation kinetics. In addition, Tz-TCO reaction provided substantially improved protein conjugation kinetics over SPAAC reaction (Fig. 4(e)), eliminating the limitation of SPAAC reaction's slow reaction rate. Taken together, the TMV-assembled microparticles yielded 2400-fold enhanced capacity over planar substrates, clearly illustrating the utility of our integrated fabrication-conjugation approach exploiting hydrogel platforms, rapid bioorthogonal reactions and biologically derived high capacity nanotemplates (i.e., TMV).

MICROSPHERE PLATFORMS WITH CONTROLLED MACROPOROUS STRUCTURES

Chang-Soo Lee's group recently reported an exciting extension of the micromolding technique to produce monodisperse polymeric microspheres by enlisting surface tension-induced droplet formation [25]. Compared with microfluidics-based microsphere fabrication approaches, this technique is considerably simple and consistent; the size of highly uniform spheres (less than 2% coefficient of variation) is readily controllable by simply changing the volume of micromolds without any complex and delicate flow controls for a wide range of diameters from 50 to 200 μm. In our most recent study, their micromolding technique was utilized to produce chitosan-PEG microspheres with quite unexpected and intriguing results [26]. As shown in the schematic diagram of Fig. 5(a), addition of hydrophobic "wetting fluid" (*N*-hexadecane) onto microwells filled with an aqueous mixture of chitosan and PEGDA leads to the formation of droplets by surface tension. Upon UV-induced photopolymerization similar to our earlier methods (Fig. 1-4), crosslinked hydrogel microspheres with uniform size are produced with near-perfect fidelity and recovery yield. The bright-field (Fig. 5(b)) and confocal micrographs upon fluorescent labeling (Fig. 5(c)-(e)) illustrate core-shell formation for a range of PEGDA content spheres, due to polymerization-induced phase separation (PIPS). Briefly, mobile polymeric and polymerizable components (chitosan and PEGDA) are pushed into the core region as the crosslinked PEG networks start occupying excluded volumes during radical polymerization from the outer regions (photoinitiator dissolved in the wetting fluid). The results on microsphere fabrication with more efficiently co-polymerizable and thus less mobile acrylate-modified chitosan support the PIPS-based core-shell structure formation; the acrylate-chitosan is mainly conjugated near sphere surfaces indicating suppressed PIPS [26]. Meanwhile, the confocal micrographs of Fig. 5(f)-(h) upon R-PE conjugation via SPAAC reaction further confirm macroporous and/or core-shell structures of the microspheres, where large R-PE molecules penetrate through the microspheres for low PEG content ones (Fig. 5(f)) or into shell layers with well-defined thickness (Fig. 5(g), (h)). These microspheres exhibit equivalent or substantially higher protein conjugation capac-

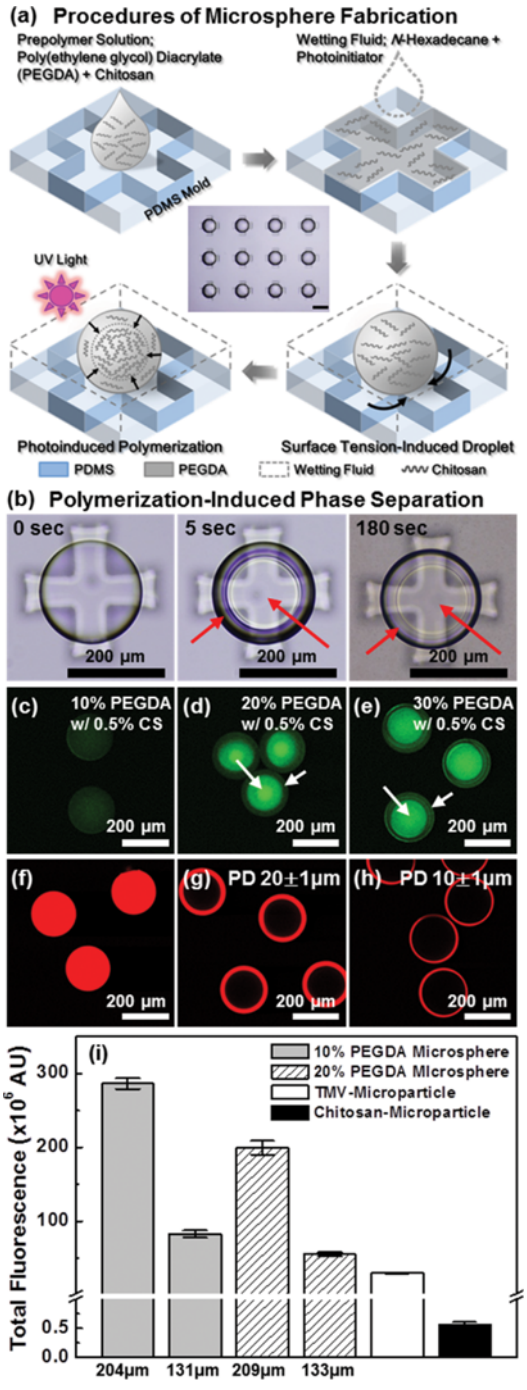

Fig. 5. Fabrication of monodisperse chitosan-PEG microspheres with controlled macroporous network structures via surface tension-induced droplet formation and PIPS. (a) Schematic diagram of the microsphere fabrication procedure. (b) Bright-field micrographs showing progress of core-shell structure formation in a prepolymer droplet during polymerization. (c)-(h) Confocal micrographs of fluorescently labeled (c)-(e) and R-PE conjugated (f)-(h) chitosan-PEG microspheres. (i) Comparison of total fluorescence intensity between R-PE conjugated chitosan-PEG microspheres with different PEG contents (gray and striped columns) and chitosan-PEG microparticles with (white column) and without TMV nanotemplates (black column). Adapted from [26]. Copyright (2015) American Chemical Society.

ity compared to TMV-assembled microparticles, as shown in the total fluorescence intensity comparison plot of Fig. 5(i). In sum, a simple micromolding-based fabrication yields chemically functional hydrogel microspheres with readily tunable and controlled network structures that can be harnessed for improved protein conjugation.

CONCLUSIONS AND FUTURE PERSPECTIVE

We have presented a concise overview of our recent efforts in the manufacturing of functional microparticles for improved biosensing performances in terms of protein conjugation capacity and kinetics via integration of micromolding, biopolymeric/supramolecular templates and bioorthogonal conjugation schemes. First, robust micromolding enables simple, clean and readily scalable routes to the fabrication of uniform microparticles or microspheres without the needs for costly equipment, delicate fabrication parameter control or tedious multistep procedures. Second, short ssDNA or chitosan provides efficient handles for self-assembly or covalent conjugation reactions for biomacro/supramolecules. Third, bioorthogonal conjugation reactions provide high yield and selective schemes for biomolecular conjugation. Our post-fabrication conjugation approach permits mild aqueous reaction conditions using stable and selective reaction intermediates, unlike other co-polymerization approaches for minimal protein damage, thus should permit extension to a large array of applications and functional microscale materials and devices. We have in fact had recent successes in employing the micromolding technique to capture catalytically active palladium nanoparticles that are templated on TMV into stable and readily deployable formats [27]. Our current efforts in further improving the biosensing capabilities and performances include incorporation of inert porogens, linear polymer matrix materials such as polyacrylamide, and other useful functional groups such as acrylic acids. We envision that such endeavors may lead to substantially higher conjugation capacity and capture kinetics, rational design principles for biosensing platforms with the performance targets tailored for specific applications, or size-selective capture and sensing of complex biological assemblies.

ACKNOWLEDGEMENTS

We extend our special gratitude to the collaborators Professor Chang-soo Lee at Chungnam National University and Dr. Changhyung Choi at Harvard University, both of who continue to provide much inspiration and support.

REFERENCES

1. K. N. Baker, M. H. Rendall, A. Patel, P. Boyd, M. Hoare, R. B. Freedman and D. C. James, *Trends Biotechnol.*, **20**, 149 (2002).
2. M. Uttamchandani, J. L. Neo, B. N. Z. Ong and S. Moochhala, *Trends Biotechnol.*, **27**, 53 (2009).
3. J. D. Wulfkuhle, L. A. Liotta and E. F. Petricoin, *Nat. Rev. Cancer*, **3**, 267 (2003).
4. A. V. Fotin, A. L. Drobyshev, D. Y. Proudnikov, A. N. Perov and A. D. MIrzabekov, *Nucleic Acids Res.*, **26**, 1515 (1998).
5. D. C. Pregibon and P. S. Doyle, *Anal. Chem.*, **81**, 4873 (2009).

6. D. A. Zubtsov, E. N. Savvateeva, A. Y. Rubina, S. V. Pan'kov, E. V. Konovalova, O. V. Moiseeva, V. R. Chechetkin and A. S. Zasedatelev, *Anal. Biochem.*, **368**, 205 (2007).
7. J. E. Meiring, M. J. Schmid, S. M. Grayson, B. M. Rathsack, D. M. Johnson, R. Kirby, R. Kannappan, K. Manthiram, B. Hsia, Z. L. Hogan, A. D. Ellington, M. V. Pishko and C. G. Willson, *Chem. Mater.*, **16**, 5574 (2004).
8. S. Park, H. J. Lee and W. G. Koh, *Sensors-Basel*, **12**, 8426 (2012).
9. B. F. Ye, Y. J. Zhao, T. T. Li, Z. Y. Xie and Z. Z. Gu, *J. Mater. Chem.*, **21**, 18659 (2011).
10. X. H. Ji, N. G. Zhang, W. Cheng, F. Guo, W. Liu, S. S. Guo, Z. K. He and X. Z. Zhao, *J. Mater. Chem.*, **21**, 13380 (2011).
11. Y. J. Zhao, H. C. Shum, H. S. Chen, L. L. A. Adams, Z. Z. Gu and D. A. Weitz, *J. Am. Chem. Soc.*, **133**, 8790 (2011).
12. J. Hu, X. W. Zhao, Y. J. Zhao, J. Li, W. Y. Xu, Z. Y. Wen, M. Xu and Z. Z. Gu, *J. Mater. Chem.*, **19**, 5730 (2009).
13. D. C. Pregibon, M. Toner and P. S. Doyle, *Science*, **315**, 1393 (2007).
14. D. C. Appleyard, S. C. Chapin, R. L. Srinivas and P. S. Doyle, *Nat. Protoc.*, **6**, 1761 (2011).
15. C. L. Lewis, C. H. Choi, Y. Lin, C. S. Lee and H. Yi, *Anal. Chem.*, **82**, 5851 (2010).
16. R. J. Meagher, J. I. Won, L. C. McCormick, S. Nedelcu, M. M. Bertrand, J. L. Bertram, G. Drouin, A. E. Barron and G. W. Slater, *Electrophoresis*, **26**, 331 (2005).
17. S. Jung and H. Yi, *Langmuir*, **28**, 17061 (2012).
18. H. Yi, L. Q. Wu, W. E. Bentley, R. Ghodssi, G. W. Rubloff, J. N. Culver and G. F. Payne, *Biomacromolecules*, **6**, 2881 (2005).
19. S. T. Koev, P. H. Dykstra, X. Luo, G. W. Rubloff, W. E. Bentley, G. F. Payne and R. Ghodssi, *Lab Chip*, **10**, 3026 (2010).
20. S. A. Agnihotri, N. N. Mallikarjuna and T. M. Aminabhavi, *J. Controlled Release*, **100**, 5 (2004).
21. F. Croisier and C. Jerome, *Eur. Polym. J.*, **49**, 780 (2013).
22. D. L. Nelson, A. L. Lehninger and M. M. Cox, *Lehninger Principles of Biochemistry*, W. H. Freeman, New York (2008).
23. S. Jung and H. Yi, *Biomacromolecules*, **14**, 3892 (2013).
24. S. Jung and H. Yi, *Langmuir*, **30**, 7762 (2014).
25. C. H. Choi, J. M. Jeong, S. M. Kang, C. S. Lee and J. Lee, *Adv. Mater.*, **24**, 5078 (2012).
26. S. Jung and H. Yi, *Chem. Mater.*, **27**, 3988 (2015).
27. C. X. Yang, C. H. Choi, C. S. Lee and H. M. Yi, *ACS Nano*, **7**, 5032 (2013).

Hyunmin Yi is currently an Associate Professor at the Department of Chemical and Biological Engineering of Tufts University in Massachusetts, U.S.A. He received his B.S. degree in Chemical Technology (Seoul National University), M.S. degree in Biochemical Engineering (Seoul National University) and Ph.D. degree in Chemical Engineering (University of Maryland at College Park), and was a postdoctoral fellow at the Center for Biosystems Research then an Assistant Research Scientist at the Department of Materials Science and Engineering, both at the University of Maryland at College Park, prior to arrival at Tufts in 2006. His research interests span broad areas of smart biomaterials, biofabrication, nanobiotechnology and biochemical engineering. Professor Yi was the recipient of KIChE President Award in 2013.